

# Narrow-line diode laser packaging and integration in the NIR and MIR spectral range

Alvaro Jimenez<sup>a</sup>, Tobias Milde<sup>a</sup>, Niklas Staacke<sup>a</sup>, Christian Assmann<sup>a</sup>, James O’Gorman<sup>bc</sup>, Joachim R. Sacher<sup>\*a</sup>, <sup>a</sup>Sacher Lasertechnik GmbH, Rudolf-Breitscheid-Str. 1-5, D-35037 Marburg, Germany, <sup>b</sup>Sensor Photonics GmbH, Rudolf-Breitscheid-Str. 1-5, D-35037 Marburg, Germany, <sup>c</sup>Xylophone Optics Ltd, Vanomer House, 191-193 Lr Kimmage Rd, Dublin 6W, Ireland

## ABSTRACT

Narrow linewidth tunable diode lasers are an important tool for spectroscopic instrumentation. Conventional external cavity diode lasers are designed as laboratory instrument and do not allow hand-held operation for portable instruments. A new miniaturized type of tunable external cavity tunable diode laser will be presented. The presentation will focus on requirements on the assembly technology of micro-optic components as well as on the physical properties of such devices. Examples for the realization of this new technology will be given in the NIR for Alkaline Spectroscopy as well as in the MIR at 1908nm.

**Keywords:** Tunable Diode Laser, GaAsP/AlGaAs Laser Diodes, GaInSb/AlGaAsSb Laser Diodes, Curved Waveguides, Volume Holographic Grating, Near Infrared, Mid Infrared, Semiconductor Device Packaging

## 1. INTRODUCTION

Tunable diode lasers are an important tool for spectroscopy over the last two decades. Starting from laboratory applications, diode lasers become more and more important for medical, pharmaceutical and industrial measurement applications. Earlier generations of diode laser systems have been limited to laboratory environments due to sophisticated, large cavity assemblies. More recent assembly technologies start to overcome these drawbacks with robust, environment insensitive technologies. A further limitation for general applications is the high cost of the laser systems. This presentation reports technology advancements, resulting into tunable, highly stable laser solutions, at a significantly reduced cost level. In Section 2, the design and the realization of novel GaAsP/AlGaAs and GaInSb/AlGaAsSb laser diode gain elements is reported. In Section 3, results of the micro-assembly of tunable diode lasers in the NIR are summarized. In Section 4, different realizations for widely tunable diode lasers in the NIR are compared. In Section 5, the realization of tunable diode lasers based on GaAsP/AlGaAs and GaInSb/AlGaAsSb laser materials is reported. Section 6 summarizes the results and provides a perspective for future developments.

## 2. LASER WAFER DESIGN AND REALIZATION

The design and manufacture of a high quality external cavity laser diode system is a complex engineering activity that requires integrated design of (i) the external cavity wavelength selection mechanisms, (ii) designed for purpose light collection and outcoupling optics, (iii) electronic actuation and control systems and finally as described in this section (iv) the laser diode gain block (chip) and its realization. Starting from previously published laser structures [1, 2], two exemplar laser diode gain block designs have been developed and will be described here; a device design in the GaAsP/AlGaAs material system providing gain in the wavelength,  $\lambda$ , interval  $760 \text{ nm} \leq \lambda \leq 800 \text{ nm}$  and a design in the GaInSb/AlGaAsSb material system providing gain in the interval  $1660 \text{ nm} \leq \lambda \leq 2100 \text{ nm}$ .

### a) GaAsP / AlGaAs Laser Diode Gain Block

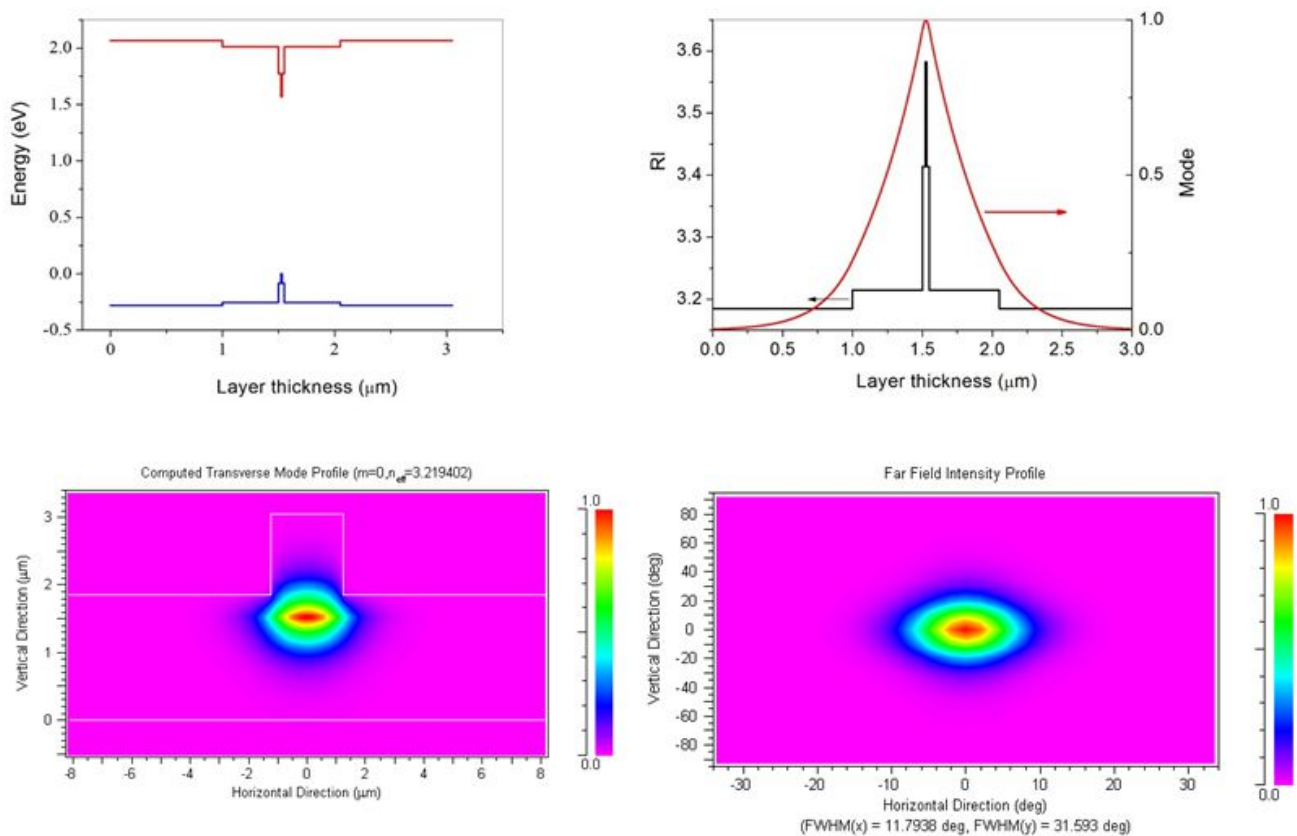
A single quantum well GaAsP high power structure designed for emission in the wavelength,  $\lambda$ , interval  $760 \text{ nm} \leq \lambda \leq 800 \text{ nm}$  was selected to provide gain. Starting from previous work This Aluminum-free material system was chosen, since it shows excellent resistance to Catastrophic Optical Damage (COD) at the expense of lasing in the TM mode.

Table 1 shows the GaAsP/AlGaAs layer structure used to fabricate the  $\lambda = 780 \text{ nm}$  gain blocks used in this work.

Layer	Description	Thickness (nm)	x	y
7	p+:GaAs contact			
6	p:AlxGa1-xAs cladding	1.5 $\mu\text{m}$	0.7	0.3
5	AlxGa1-xAs waveguide	0.5 $\mu\text{m}$	0.65	0.35
4	GaAsP QW	9 nm		
3	n:AlxGa1-xAs waveguide	0.5 $\mu\text{m}$	0.65	0.35
2	n:AlxGa1-xAs cladding	2 $\mu\text{m}$	0.7	0.3
1	n:GaAs buffer			
	n:GaAs substrate			

**Table 1: Layer structure of the GaAsP/AlGaAs laser diode [3] used in this paper.**

Figure 1 illustrates Optical Simulations of Beam Propagation in the waveguide structure of Table 1. Good optical confinement to the ridge waveguide is seen in the transverse directions while the propagating modes shows excellent overlap with the GaAsP quantum well.



**Figure 1: Optical Simulations of Beam Propagation in the GaAsP/AlGaAs waveguide structure of Table 1.**

The calculated farfield intensity profile is elliptical with a far field beam profile of  $12^\circ \times 31.6^\circ$  FWHM. Having calculated the beam propagation parameters, they are incorporated into a commercial laser model that uses the Rsoft simulation package. The laser parameters used in this calculation are:

<b>LASER PARAMETERS</b>	
Length, $L$	1mm
Ridge waveguide width, $w$	$3\mu\text{m}$
Front facet reflectivity, $R_f$	5%
Back facet reflectivity, $R_b$	95%
Internal loss, $\alpha_{int}$	$5\text{cm}^{-1}$

**Table 2 Laser parameters used in laser simulations**

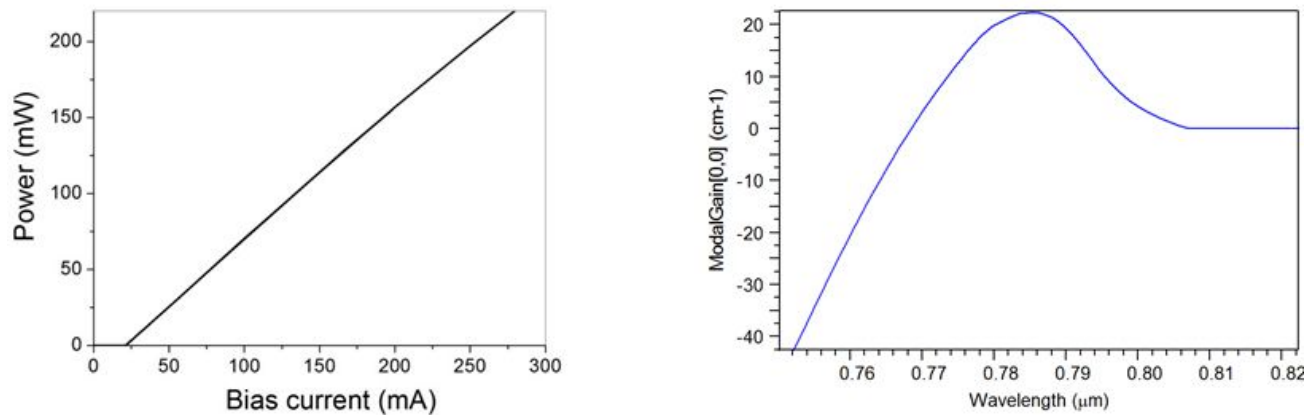


**Figure 2: Optical Simulations of the performance of the GaAsP/AlGaAs laser diode structure of Table 1.**

Figure 2 shows optical simulations of the performance of the GaAsP/AlGaAs laser diode structure of Table 1. An excellent threshold current ( $I_{th} \sim 25$  mA) is calculated for this high emission power ( $P_{out} \sim 200$  mW) laser diode. This when taken together with the superb laser far field of Figure 1 and the wide calculated gain curve of Figure 2(b), bodes well for its performance as a gain block in an external cavity laser.

A number of key parameters must be optimised to optimise the gain block performance. These include laser cavity length, facet reflectivities and internal losses. A range of simulations were carried out varying these parameters in order to understand the effect of change in these parameters. These results are shown in Figure 3 for a range of laser diode cavity lengths and front facet reflectivities of (a)  $R_f = 1\%$ , (b)  $R_f = 5\%$ , (c)  $R_f = 10\%$  and (d)  $R_f = 20\%$ .

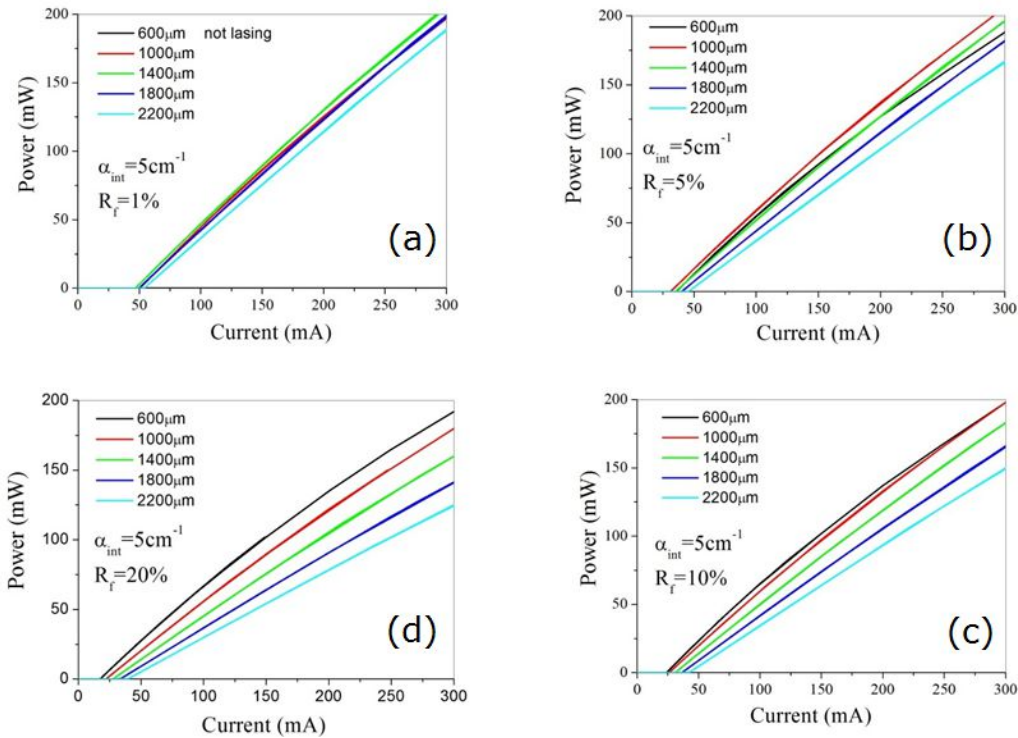


**Figure 3: Calculated laser characteristics exhibiting the impact of key parameters on laser performance.**

From these simulations, it is apparent that the optimum laser diode device geometry for an emission power of approximately 100mW is:

- Cavity length  $\sim 1200\mu\text{m}$
- $R_f = 5\%$
- Ridge waveguide width  $3\mu\text{m}$

In external cavity laser diodes, the interior facet is antireflection coated to reduce or preferably eliminate sub-cavity etalon effects. Figure 4 illustrates the impact of sub-cavity etalons on the spectral selectivity of the external cavity where the residual laser diode Fabry-Pérot modes interact with the reflection curve of an external cavity grating tuning element. For the optimised parameters of Figure 3, Figure 4 (a) tabulates the laser diode sub-cavity mode spacing. While Figure 4(b) illustrates the interaction of the sub-cavity modes with the grating reflection spectrum.

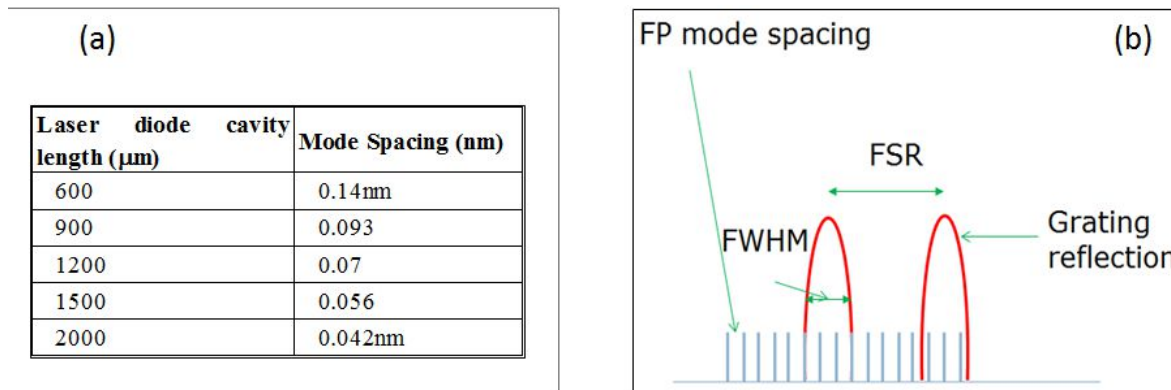


**Figure 4: Impact of laser diode sub-cavity etalons on spectral selectivity of an external cavity laser diode.**

It is clear that a hyper-low antireflection coating is required on the interior laser facet to get the best external cavity laser diode performance in terms of mode hop free emission wavelength tuning over the full wavelength tuning curve allowed by the diode gain curve. The best way to achieve this is to angle the guiding ridge [4, 5] at the interior facet in the course of device fabrication and prior to facet antireflection coating as illustrated in Figure 5. This layout allows the chip segment to be conveniently cleaved into devices of length  $L = 600 \mu\text{m}$ ,  $1200 \mu\text{m}$  and  $1800 \mu\text{m}$  to evaluate the best gain chip length.

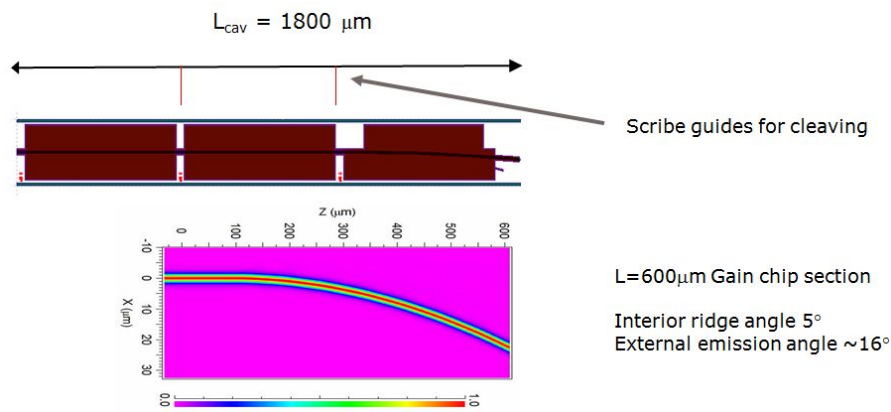


Figure 5: Chip schematic and waveguide for an angled facet gain chip.

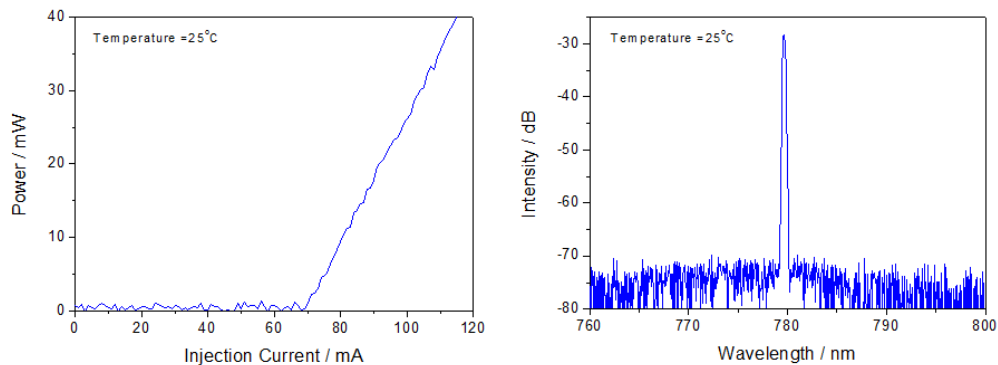


Figure 6: Initial performance data for a  $\lambda = 780\text{nm}$  tunable external cavity laser diode.

Figure 6 shows initial test data for an external cavity laser diode emitting in a single mode at  $\lambda = 780 \text{ nm}$ . A linear light current curve with  $I_{\text{th}} = 70 \text{ mA}$  is measured. The device threshold current and differential quantum efficiency agree well with the calculated performance shown in Figure 3 (c), particularly the  $L_{\text{cav}} = 1400 \mu\text{m}$  data.

b) *GaInSb / AlGaAsSb laser diode gain block*

We have also developed 3 quantum well GaInSb/AlGaAsSb high power laser diode structures for the implementation of tuneable laser diodes emitting around  $\lambda = 1900 \text{ nm}$  and  $\lambda = 2020 \text{ nm}$ . The quantum well layer structure of the  $\lambda = 1900 \text{ nm}$  structure is given in Table 3.

Layer	Description	Thickness (nm)	Material	x	y
23	Cap	100	GaSb		
22	graded	50	Al <sub>x</sub> Ga <sub>1-x</sub> As <sub>y</sub> Sb <sub>1-y</sub>	0.5 - 0	
21	p cladding	200	Al <sub>x</sub> Ga <sub>1-x</sub> As <sub>y</sub> Sb <sub>1-y</sub>	0.5	0.04
20	p cladding	200	Al <sub>x</sub> Ga <sub>1-x</sub> As <sub>y</sub> Sb <sub>1-y</sub>	0.5	0.04
19	p cladding	1000	Al <sub>x</sub> Ga <sub>1-x</sub> As <sub>y</sub> Sb <sub>1-y</sub>	0.5	0.04
18	p cladding	200	Al <sub>x</sub> Ga <sub>1-x</sub> As <sub>y</sub> Sb <sub>1-y</sub>	0.5	0.04
17	p cladding	200	Al <sub>x</sub> Ga <sub>1-x</sub> As <sub>y</sub> Sb <sub>1-y</sub>	0.5	0.04
16	p cladding	100	Al <sub>x</sub> Ga <sub>1-x</sub> As <sub>y</sub> Sb <sub>1-y</sub>	0.5	0.04
15	p cladding	100	Al <sub>x</sub> Ga <sub>1-x</sub> As <sub>y</sub> Sb <sub>1-y</sub>	0.5	0.04
14	graded	50	Al <sub>x</sub> Ga <sub>1-x</sub> As <sub>y</sub> Sb <sub>1-y</sub>	0.3 - 0.5	
13	p waveguide	100	Al <sub>x</sub> Ga <sub>1-x</sub> As <sub>y</sub> Sb <sub>1-y</sub>	0.3	0.02
12	QW	10	Ga <sub>1-x</sub> In <sub>x</sub> Sb		
11	barrier	20	Al <sub>x</sub> Ga <sub>1-x</sub> As <sub>y</sub> Sb <sub>1-y</sub>	0.3	0.02
10	QW	10	Ga <sub>1-x</sub> In <sub>x</sub> Sb		
9	barrier	20	Al <sub>x</sub> Ga <sub>1-x</sub> As <sub>y</sub> Sb <sub>1-y</sub>	0.3	0.02
8	QW	10	Ga <sub>1-x</sub> In <sub>x</sub> Sb		
7	n waveguide	100	Al <sub>x</sub> Ga <sub>1-x</sub> As <sub>y</sub> Sb <sub>1-y</sub>	0.3	0.02
6	graded	50	Al <sub>x</sub> Ga <sub>1-x</sub> As <sub>y</sub> Sb <sub>1-y</sub>	0.5 - 0.3	
5	n cladding	500	Al <sub>x</sub> Ga <sub>1-x</sub> As <sub>y</sub> Sb <sub>1-y</sub>	0.5	0.04
4	n cladding	500	Al <sub>x</sub> Ga <sub>1-x</sub> As <sub>y</sub> Sb <sub>1-y</sub>	0.5	0.04
3	n cladding	1000	Al <sub>x</sub> Ga <sub>1-x</sub> As <sub>y</sub> Sb <sub>1-y</sub>	0.5	0.04
2	graded	50	Al <sub>x</sub> Ga <sub>1-x</sub> As <sub>y</sub> Sb <sub>1-y</sub>	0 - 0.5	
1	buffer	150	GaSb		
GaSb substrate Te doped					

**Table 3: Layer structure for 3 quantum well GaInSb / AlGaAsSb laser diode fabrication**

Two laser structures were grown on 3-inch wafers substrates by MBE one for emission at  $\lambda = 1900$  nm, the other for emission around  $\lambda = 2020$  nm. This report will primarily concern the laser diode structures emitting at wavelength  $\lambda = 1900$  nm and their performance. Figure 7, however, shows measured Photoluminescence (PL) for the two structures grown and the expected tuning range from devices exhibiting such emission. The measured PL wavelength peaks are at  $\lambda = 1896$  nm and  $\lambda = 2019$  nm. The high PL intensities indicate high quality laser structures with low defect densities.

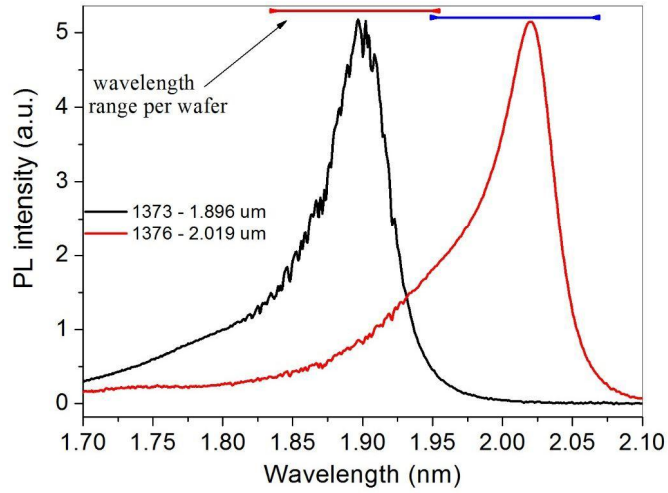


Figure 7: Measured Photoluminescence (PL) for the two GaInSb laser structures used in this work and the expected tuning range from devices exhibiting such emission

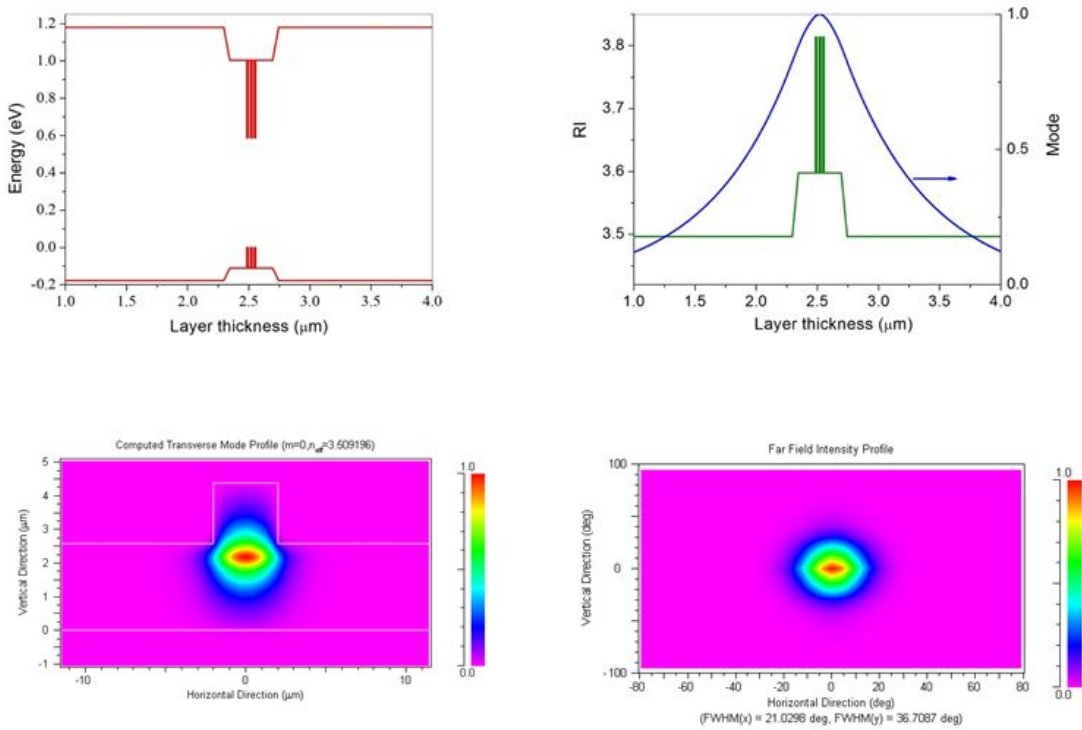
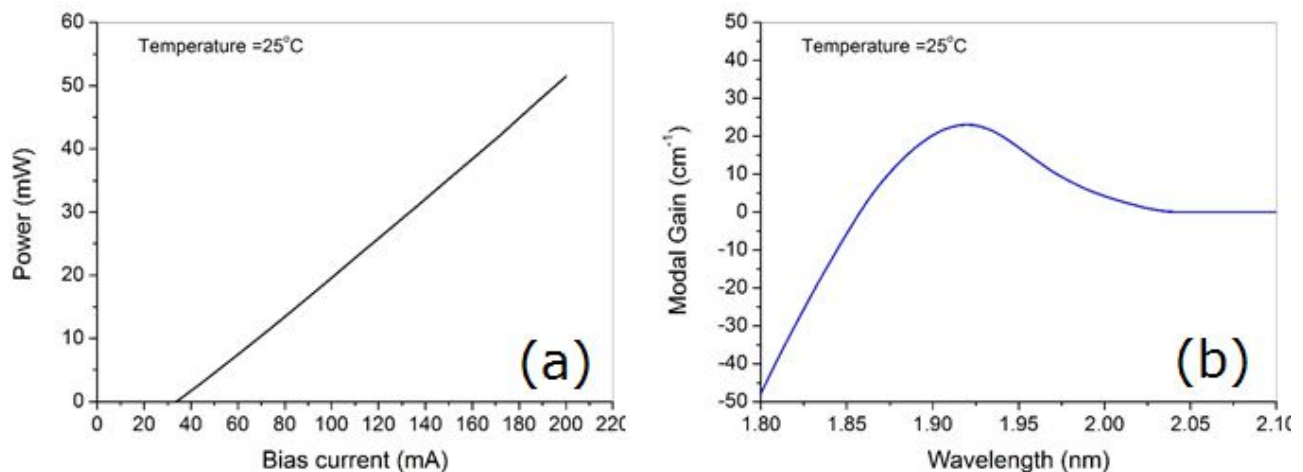


Figure 8: Optical Simulations of Beam Propagation in the GaInSb/AlGaAsSb waveguide structure of Table 3.

Figure 8 illustrates Optical Simulations of Beam Propagation in the waveguide structure of Table 3. Good optical confinement to the ridge waveguide is seen in the transverse directions. The calculated farfield intensity profile is elliptical with a far field beam profile of  $21^\circ \times 37^\circ$  FWHM. Having calculated the beam propagation parameters, they are incorporated into a commercial laser model that uses the Rsoft simulation package. The laser parameters used in this calculation are:

<b>GaInSb / AlGaAsSb LASER PARAMETERS</b>	
Length, $L$	$900 \mu\text{m}$
Ridge waveguide width, $w$	$3 \mu\text{m}$
Front facet reflectivity, $R_f$	10 %
Back facet reflectivity, $R_b$	95 %
Internal loss, $\alpha_{int}$	$7 \text{ cm}^{-1}$

**Table 4: Laser parameters used in laser simulations**



**Figure 9: Optical Simulations of the performance of the GaInSb/AlGaAsSb laser diode structure of Table 3.**

Figure 9 shows optical simulations of the performance of the GaInSb / AlGaAsSb laser diode structure of Table 4. An excellent threshold current ( $I_{th} \sim 32 \text{ mA}$ ) is calculated for this high emission power ( $P_{out} \sim 50 \text{ mW}$ )  $\lambda = 1.9 \mu\text{m}$  emission wavelength laser diode. This when taken together with the superb laser far field of Figure 8 and the wide calculated gain curve of Figure 9(b), bodes well for its performance as a gain block in an external cavity laser.

Again, a number of key parameters must be optimised to optimise the GaInSb / AlGaAsSb gain block performance. Once again these include laser cavity length, facet reflectivities and internal losses. A range of simulations were carried out varying these parameters in order to understand the effect of change in these parameters. These results are shown in Figure 10 for a range of laser diode cavity lengths  $L_{cav} = 400 \mu\text{m}$ ,  $600 \mu\text{m}$  and  $900 \mu\text{m}$  and front facet reflectivities of (a)  $R_f = 5\%$ , (b)  $R_f = 10\%$ , (c)  $R_f = 20\%$  and (d)  $R_f = 30\%$ .

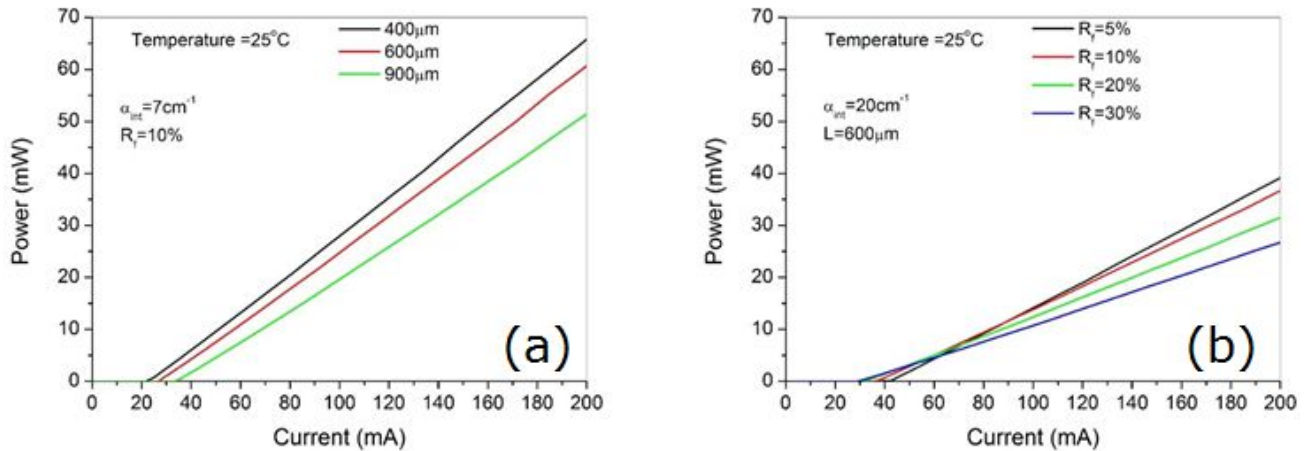


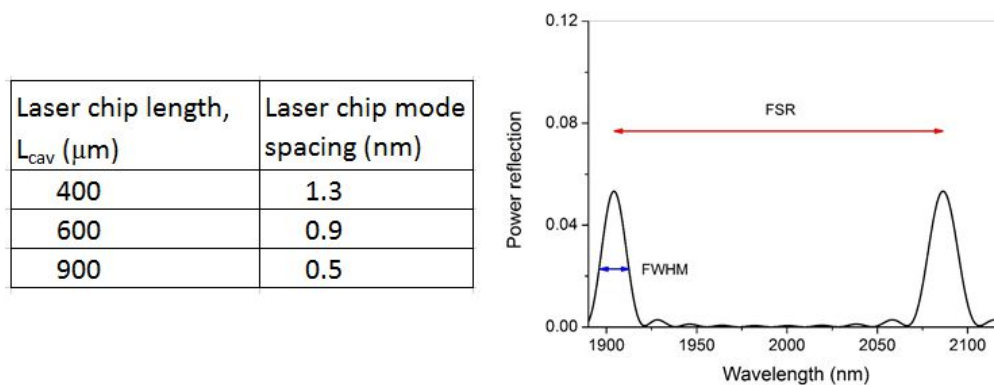
**Figure 10: Calculated laser characteristics exhibiting the impact of key parameters on laser performance.**

From these simulations, it is apparent that the optimum GaInSb / AlGaAsSb laser diode device parameters for an emission power of ~ 30mW are:

Optimum device parameters	
$R_f$	10%
Cavity Length	500 $\mu\text{m}$
Ridge waveguide width	3 $\mu\text{m}$

**Table 5: Calculated optimum GaInSb / AlGaAsSb device parameters**

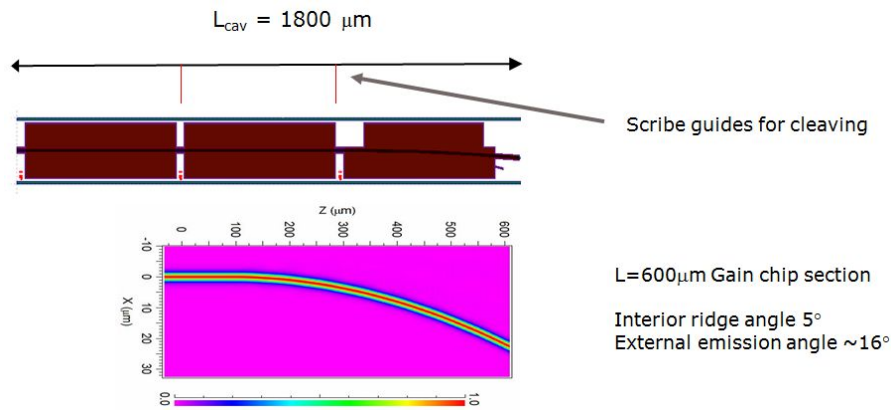
In external cavity laser diodes, the interior facet is antireflection coated to reduce or preferably eliminate sub-cavity etalon effects. Figure 11 illustrates the impact of sub-cavity etalons on the spectral selectivity of the external cavity where the residual laser diode Fabry-Pérot modes interact with the reflection curve of an external cavity grating tuning element. For the optimised parameters of Table 5, Figure 11 tabulates the GaInSb / AlGaAsSb laser diode sub-cavity mode spacing and also illustrates the interaction of the sub-cavity modes with the grating reflection spectrum.



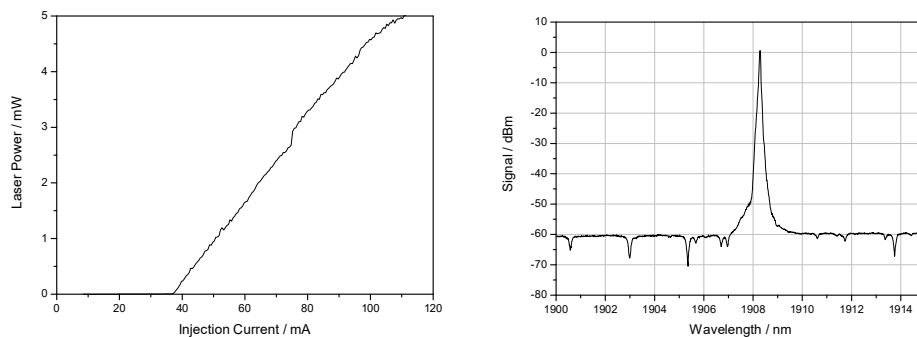
**Figure 11: Impact of laser diode sub-cavity etalons on spectral selectivity of an external cavity laser diode.**

Again as in the case of the GaAsP/AlGaAs devices it is clear that a hyperlow antireflection coating is required on the interior laser facet to get the best external cavity laser diode performance in terms of mode hop free emission wavelength tuning over the full wavelength tuning curve allowed by the diode gain curve. The best way to achieve this is to angle the guiding ridge [4, 5] at the interior facet in the course of device fabrication and prior to device facet coating as

illustrated in Figure 12. Again, the gain chip can be conveniently cleaved into devices of length  $L = 600 \mu\text{m}$ ,  $1200 \mu\text{m}$  and  $1800 \mu\text{m}$  to evaluate the best gain chip length.



**Figure 12: Chip schematic and waveguide for an angled facet gain chip.**



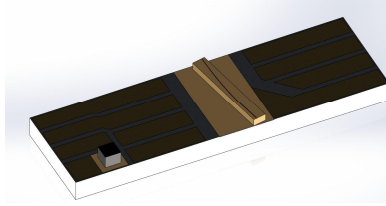
**Figure 13 Initial performance data for a  $\lambda = 1908\text{nm}$  tunable external cavity laser diode. The narrow dips in the spectrum are caused by water vapor absorption within the detection setup.**

Figure 13 shows initial test data for an external cavity laser diode emitting in a single mode at  $\lambda = 1908 \text{ nm}$ . A linear light injection current curve with  $I_{th} = 35 \text{ mA}$  is measured. The device threshold current agrees well with the calculated performance shown in Figure 10 (b). It is to be noted that the laser shows significant thermal saturation which impacts the emission power at high drive currents.

The next step after the design of the laser diode gain chip is the assembly of the gain chip together with optical components for defining the features of the laser device.

### 3. MICRO-ASSEMBLY LASER OF TUNABLE NIR DIODE LASERS

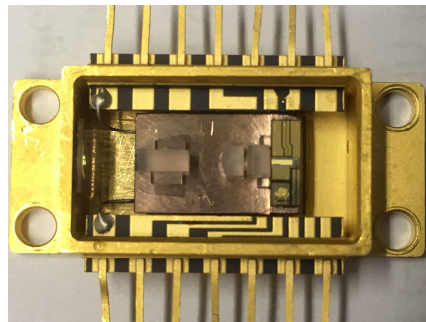
The micro-assembly requires specific components, different from conventional external cavity diode lasers. Mounting platform is a micro-bench for mounting diode laser gain chip, collimating lenses, and wavelength selective element for providing feedback. The micro-bench is mounted to a thermos-electric cooler inside of a protective housing. However, commercially available diode laser gain chips are mostly mounted into 9mm TO packages or to so-called c-blocks which are not compatible with a compact layout.



**Figure 14. Diode Laser Gain Chip and Temperature Sensor mounted to AlN Subcarrier.**

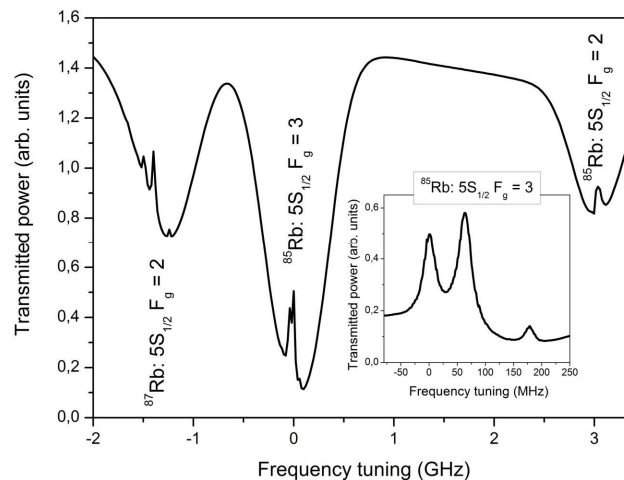
A specific AlN subcarrier was designed for integrating the diode laser gain chip into the micro-bench. Figure 14 shows a schematic of the realization of the subcarrier with soldered gain chip and NTC type of thermistor.

The assembly begins with soldering the diode laser gain chip to the micro-bench and mounting the micro-bench into the protective housing. The diode laser gain chips are connected electrically and operated during the further assembly. As next steps, fast axis collimating lens (FAC) and slow axis collimating lens (SAC) are positioned and optimized by *in-situ* monitoring the resulting beam profile. After finishing the collimation, the Volume Holographic Grating (VHG) as wavelength selective element is integrated into the micro-bench. The position is optimized via *in-situ* monitoring of the laser performance prior to fixing the wavelength selective element.



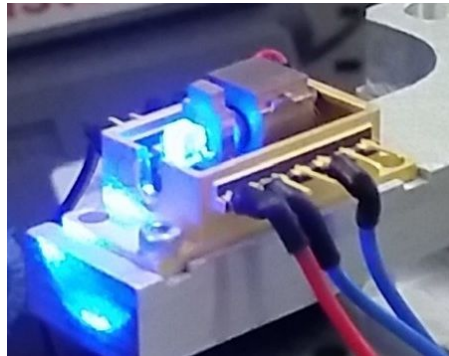
**Figure 15. Assembled Micro-External Cavity Diode Laser**

Figure 15 shows an example of an assembled micro-external cavity diode laser, consisting of diode laser gain chip mounted to subcarrier, FAC; SAC and VHG. Typical performance data are 6 GHz mode-hop free tuning, < 20kHz linewidth, <135dB/Hz RIN, and up to 380 mW output power [8].



**Figure 16. Doppler free absorption of the D2 transition of Rubidium**

In case of a laser system for a specific application, like the Doppler-free absorption structure of the D2 transition of Rubidium, the laser performance is verified via an *in-situ* measurement of the D2 absorption line of Rubidium as shown in Figure 16, prior to fixing the VHG at its final position.



**Figure 17: VHG laser at 461nm for Strontium Cooling**

The concept of the Micro-External Cavity Diode Laser was realized for the most commonly used Alkaline Atom absorption lines, like Rubidium D1 and D2 transition, Cesium D1 and D2 transition, Potassium [14] and others atoms as Strontium which require only small tuning range in the order of 5GHz to 10GHz. Figure 17 shows the realization of a 461nm VHG laser for Strontium cooling.

VHG lasers have also been realized for the applications in molecular spectroscopy like Oxygen Absorption at 761.14nm and Water Vapor at 1396.6nm. However, the concept shows limitations with these applications since the tuning range only covers one line of the absorption bands. A larger tuning range is required for a proper identification of the molecular transition. Therefore, concepts for expanding the tuning range into the nanometer range have been evaluated.

#### **4. WIDE TUNABLE MICRO-ASSEMBLED LASER OF NIR TUNABLE DIODE LASERS**

Different NIR tunable diode laser concepts have been developed and tested. Within these concepts, there are two outstanding options which have shown interesting results for a tunable laser. In first place, a transversely chirped volume holographic grating (VHG) was employed to stabilize and tune an external cavity diode laser (ECDL). In order to tune the laser, the VHG was laterally translated to select the stabilized frequency. The second option was to employ a transmission grating as a spatial filter for the external cavity. In this case, tuning was made through a tilting mirror. Both concepts, together with their integration capabilities, will be explained in detail in the following paragraphs.

##### **4.1 Broadly tunable Chirped Volume Holographic Bragg Grating diode laser**

In order to achieve a continuously tunable, compact, single-mode diode laser, an approach via a transmitting chirped Volume Holographic Bragg Grating is proposed. Compared to narrowband Bragg gratings, the transverse chirp allows the extension of the tuning while keeping a narrow linewidth. ECDLs in Littrow or Littman-Metcalf configurations [6] are sensible to acoustic and temperature variations, problems which are overcome by a compact integration of the grating within an external cavity setup.

The system is composed of a ridge waveguide emitting (RWE) laser, fast and slow axis collimating lenses and a VHBG. The laser diode (LD) chip employed is 1200  $\mu\text{m}$  long and includes an InGaAs triple quantum well (TQW) active region. It is soldered on an AlN submount, which has been placed together with the collimating lenses on a copper micro-bench which is temperature stabilized to 22  $^{\circ}\text{C}$ . For collimation, aspherical cylindrical lenses have been employed with focus lengths of 1 mm and 2.5 mm respectively for the fast and slow axis. A transmitting chirped VHBG recorded in photo-thermo-refractive glass (PTR-glass) has been employed as high efficiency, low loss intracavity filter in order to achieve a high beam quality [7, 8]. The anti-reflection (AR) coated VHBG, placed at a distance of 5 cm from the LD, is centered around 1059 nm and reflects back 54% of the incoming intensity back into the LD. Figure 18 shows the setup in which tuning is achieved by a translation of the Bragg grating.

The VHBG is transversely chirped, which means it has a fan-shaped grating structure to obtain tuning of the signal wavelength by linearly translating the grating. This tuning method has previously been used for distributed feedback dye

[9] and semiconductor [10] lasers. The resulting VHBG has a spectral selectivity of 0.59 nm while the whole tuning range is in excess of 10 nm, from 1053 to 1064.1 nm.

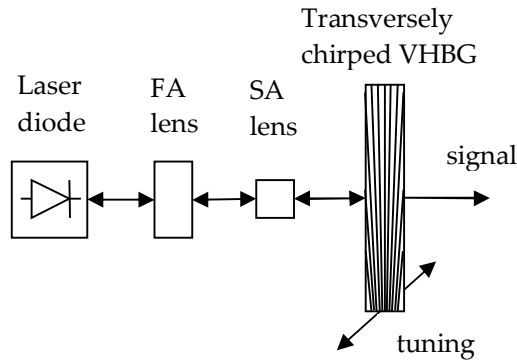


**Figure 18: Broadly tunable chirped volume holographic grating system setup. Tuning is achieved by diagonal translation of the VHG.**

The optical spectrum of the setup in Figure 18 was measured by fiber coupling the signal after the beam has passed an optical isolator and recording it with the help of an optical spectrum analyzer. The threshold current from the device configured at the central wavelength of the VHBG, 1060 nm, is of 55 mA. The maximum power obtained from the system was of 29.5 mW at a gain current of 120 mA. In order to show the maximum tuning span of the experimental setup, the VHBG was mounted on a three-axis linear stage and swept perpendicularly over the whole range allowed by the translation stage, 5 mm. With this displacement, a tuning of 4.11 nm was achieved at a rate of 0.822 nm/mm as shown in Figure 2.

The key objective of this setup is to achieve the broadest possible mode-hop free tuning. When translating the grating in a perpendicular way to the laser diode, the system presents mode hops between the modes of the cavity. These modes are fixed due to the constant size of the cavity. However, if the grating is moved diagonally while maintaining it perpendicular to the laser diode, as sketched in Figure 1, a better mode matching within the cavity can be achieved. Figure 3 shows a totally mode-hop free tuning range larger than 0.3 nm while moving the translation stage at an angle of 60 degrees with respect to the laser beam.

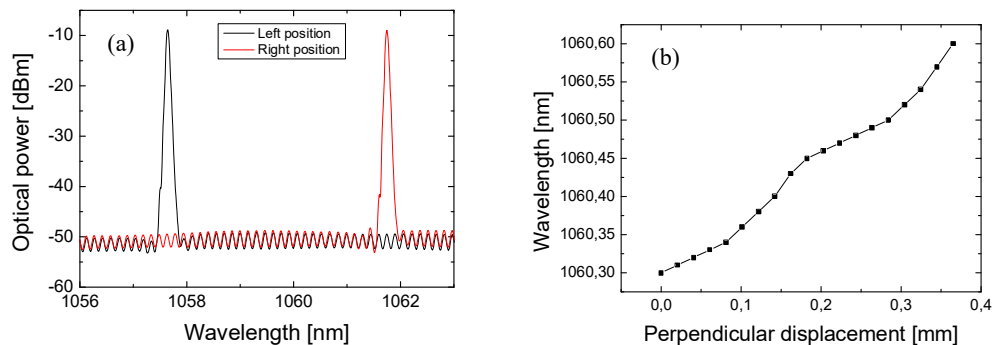


**Figure 19: Spectral behavior of the chirped VBG laser diode setup: (a) High tunability span of the chirped VHG of 4.11nm at the opposite position of the translation stage and (b) Mode-hop free tuning range of 0.3nm while diagonally tuning the chirped VBG**

Compared to non-chirped Bragg grating setups, the tuning range is dramatically increased while keeping a compact approach to the whole system. Furthermore, VHBGs can be easily adapted to different wavelengths in a very broad spectrum. Along with the presented reproducible wavelength tunability it thus is an ideal candidate for mobile operation.

In terms of integration, the VHBG offers some benefits and drawbacks. While the broad tuning range offers a big flexibility in order to select the desired frequency, in order to make use of the whole tuning range it is necessary to employ a highly stable linear translation stage. The miniaturization of the package, which is one of the key aspects of this paper, is compromised in order to obtain a high tuning range as a tradeoff parameter. However, this issue can be overcome by fixing the VHBG in the mounting process. In this way, the central wavelength of the ECDL can be selected freely in the mounting process in order to address very specific absorption lines without having the tolerance issues which are present in the usual narrowband volume Bragg gratings. The result will be a tolerance-free wavelength selection in the production of the ECDLs.

#### **4.2 MEMs tunable diode laser via transmission grating**

A concept to create a tunable diode laser is presented with the implementation of a setup including a transmission grating as a filtering element and a tilting mirror to tune the diode laser in an external cavity configuration. The tilting mirror is controlled by a Micro Electro Mechanical (MEM) actuator, which ensures a compact packaging. MEMS are nowadays a driver for the commercial development of optical systems due to cost effective manufacturability and scalability [11] as the processes are derived from a very mature silicon technology. The application of MEMs related to light includes a wide variety such as confocal microscopy, bar code reading or finger print sensing [12, 13]. In this article, their application to create a widely tunable laser diode is presented. While keeping a very compact device size, a very broad tuning range is achieved while keeping excellent power, beam and tuning behaviors. Compared to the previously presented VHBG tunable laser diode concept, the concept including a transmission grating and a MEM actuator boosts significantly the laser characteristics without the need of a bulky translation stage and even increases the tuning range of the system, which will be only limited by the gain bandwidth of the laser diode.

The system is composed of a ridge waveguide emitting (RWE) laser, fast and slow axis collimating lenses, a transmission grating and a tilting mirror. The laser diode chip employed includes a GaAs quantum well active region. As well as the chip used for the VHBG setup, it is soldered on an AlN submount placed together with the collimating lenses in the same kind of copper micro-bench stabilized at 22 °C. Similar cylindrical lenses are used to collimate the fast and slow axis independently. The transmission grating is fabricated on Schott B270 substrate and disperses the incident light on the opposite side of the grating at a wavelength dependent angle. A silver coated mirror with reflectance higher than 96% at the wavelength of interest closes the cavity, feeding back the light from the 1<sup>st</sup> order diffracted by the transmission grating. This 1<sup>st</sup> order represents a 10% of the incident light, having the rest of the power in the output represented by the 0<sup>th</sup> order, or transmitted beam, of the grating due to a blaze angle employed to minimize the power losses in 2<sup>nd</sup> and higher diffraction orders. Figure 20 shows the setup for the MEMs tunable diode laser via transmission grating.

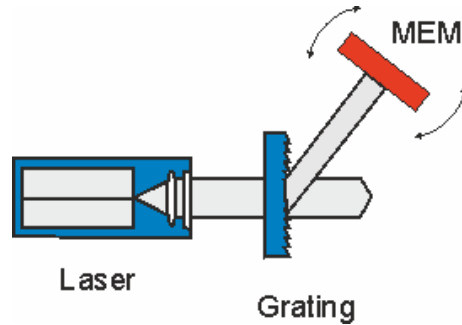


**Figure 20: MEMs tunable diode laser via transmission grating system setup. Tuning is achieved by tilting of the mirror located on the MEM actuator.**

This setup shows an excellent tuning performance. Figure 21 shows the recorded optical spectrum through the whole gain bandwidth offered by the gain chip, as there was no limitation induced by the mirror tilting or the grating. The optical spectrum was recorded after a 55 dB free space isolator with a constant current of 200 mA, reaching a maximum output power of 67.3 mW. The wavelength can be tuned from 750 nm up to 793 nm, which extends the tuning span of the current commercially available tunable lasers in an extremely compact and stable packaging. Furthermore, with the inclusion of the MEMS actuator, no bulky mechanic pieces are needed. The control of the mirror's tilt can be remotely managed through the application of a voltage signal.

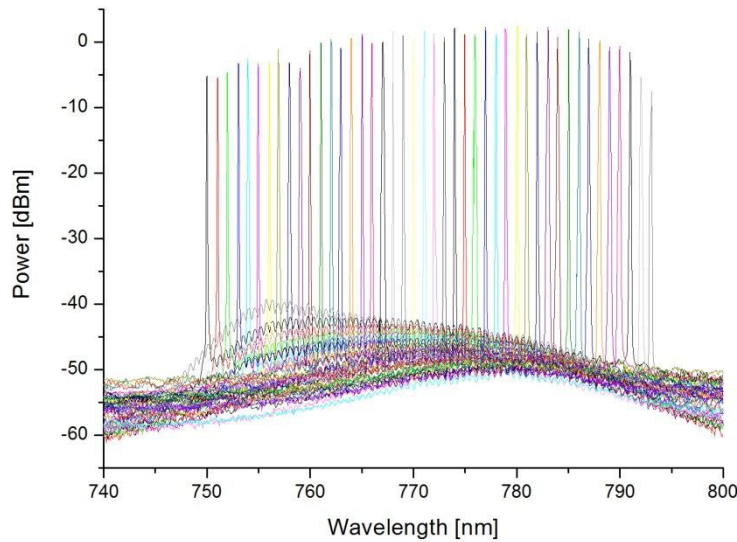


**Figure 21: Tuning range of the MEMs tunable diode laser via transmission grating system setup.**

The presented setup of tunable laser offers promising results. This technology has demonstrated an excellent tunability together with high output power. It can be exported to any wavelength range and relies in compact and inexpensive parts, providing portable and stable devices.

## 5. MICRO-ASSEMBLY LASER OF TUNABLE MIR DIODE LASERS

For MIR tunable diode laser, the previously discussed material system GaInSb/AlGaAsSb was applied. GaInSb/AlGaAsSb is advantageous over InP based materials due to its higher gain above 1.9 $\mu\text{m}$ . Figure 22 shows a technical realization of a miniaturized Littman type of external cavity diode laser.

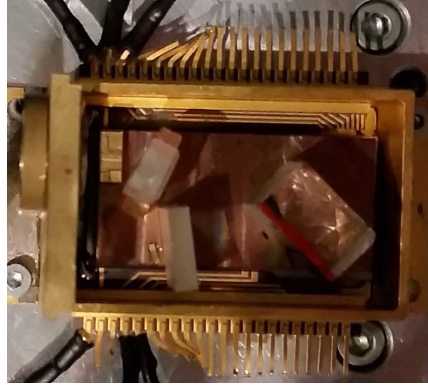


Figure 22: Realization of a tunable external cavity diode laser at 1908nm, based on a Littman cavity

A wavelength of  $\lambda = 1908\text{nm}$  was chosen due to an atmospheric transmission gap for outer space observations.

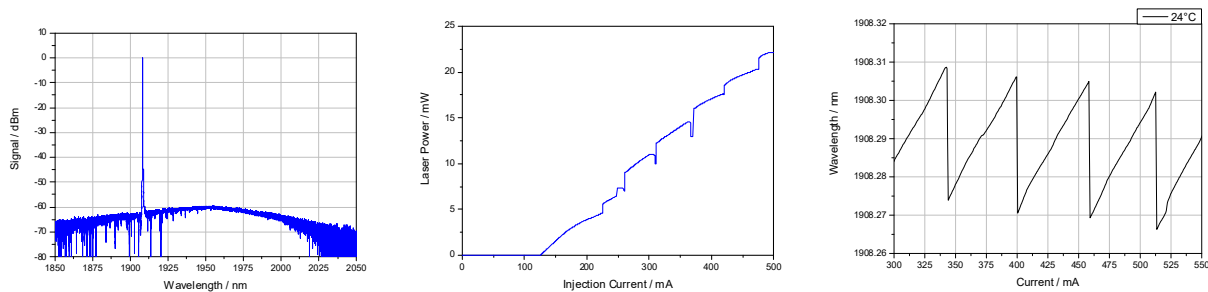
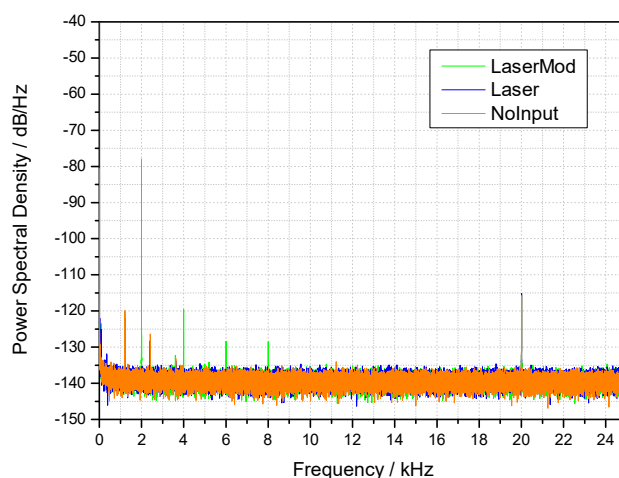


Figure 23: Initial performance data for a  $\lambda = 1908\text{nm}$  tunable external cavity laser diode.

The left-hand graph of Figure 23 shows the optical spectrum at  $\lambda = 1908\text{nm}$ . The center graph shows the laser power injection current characteristic. The right-hand graph of Figure 23 shows the tuning behavior around  $\lambda = 1908\text{nm}$  as function of the injection current at 24°C. The laser system is stabilized to a wavemeter for achieving a long-term stability of better than 30MHz.



**Figure 24: Power Spectral Density operated at  $\lambda = 1908\text{nm}$**

For technical application, the power spectral density (PSD) is of significant importance. Figure 25 shows the PSD under various conditions. The orange curve shows the signal of the detection setup. The blue curve shows the PSD with operated laser. The green curve shows the PSD with a reference modulation.

The reported technology is also applicable for the important Carbon dioxide absorption band in the 2004nm regime as well as to the water vapor absorption band in the 1866nm regime.

## 6. SUMMARY

State of the art production technologies require instantaneous detection systems with high power and narrow linewidth laser systems. Conventional types of external cavity diode lasers are bulky and sensitive to ambient conditions. A new concept for miniaturized external cavity diode lasers was reported. Due to the non-availability of gain chips with a matching housing and performance, gain chips have been developed. This presentation summarizes the steps of the development of GaAs as well as GaSb based gain chips. The assembly of the gain chips to fully operational external cavity diode laser as well as their performance data are reported. Concepts for designing and realizations of tunable miniaturized external cavity diode lasers are presented. Future work will expand the technology into the MIR spectral regime, based on Interband Cascade Lasers as well as based on Quantum Cascade Lasers.

The authors gratefully acknowledge financial support thru the German government (BMBF) within contract 13N13402, 13N13822, and 13N13823.

## REFERENCES

- [1] O. Brox ; Frank Bugge ; A. Mogilatenko ; E. Luvsandamdin ; A. Wicht, et al. " Small linewidths 76× nm DFB-laser diodes with optimised two-step epitaxial gratings ", *Proc. SPIE* 9134, Semiconductor Lasers and Laser Dynamics VI, 91340P (May 2, 2014); doi:10.1117/12.2052914; <http://dx.doi.org/10.1117/12.2052914>
- [2] Gregory Belenky ; Dimitri Donetski ; Leon Shterengas ; Takashi Hosoda ; Jianfeng Chen, et al. "Interband GaSb-based laser diodes for spectral regions of 2.3-2.4  $\mu\text{m}$  and 3-3.1  $\mu\text{m}$  with improved room-temperature performance", *Proc. SPIE* 6900, Quantum Sensing and Nanophotonic Devices V, 690004 (February 01, 2008); doi:10.1117/12.754713; <http://dx.doi.org/10.1117/12.754713>

- [3] G. Erbert, F. Bugge, A. Knauer, J. Sebastian, A. Thies, H. Wenzel, M. Weyers, G. Tränkle, High-Power Tensile-Strained GaAsP–AlGaAs Quantum-Well Lasers Emitting Between 715 and 790 nm, *IEEE J. Selected Optics in Quantum Electronics*. 5, 780 – 784 (1999)
- [4] C. F. Lin and C-S Juang, “Superluminescent Diodes with Bent Waveguide”, *IEEE Phot Tech Letts* 8 (2), 206 – 208 (1996)
- [5] Sławomir Sujecki; Eric C. Larkins “Bent waveguide laser cavities” *Proc. SPIE 5958, Lasers and Applications*, 59580W (12 October 2005)
- [6] M. G. Littman and H. J. Metcalf, “Spectrally narrow pulsed dye laser without beam expander,” *Appl. Opt.* 17, 2224–2227 (1978).
- [7] Jacobsson, B.; Pasiskevicius, V.; Laurell, F.; Smirnov, V.; Glebov, L., "Tunable optical parametric oscillator controlled by a transversely chirped Bragg grating," in *Lasers and Electro-Optics, 2008 and 2008 Conference on Quantum Electronics and Laser Science. CLEO/QELS 2008. Conference on*, vol., no., pp.1-2, 4-9 May 2008
- [8] Rauch, S.; Sacher, J., "Compact Bragg Grating Stabilized Ridge Waveguide Laser Module With a Power of 380 mW at 780 nm," in *Photonics Technology Letters, IEEE*, vol.27, no.16, pp.1737-1740, Aug.15, 15 2015
- [9] A. Matsuda and S. Iizima, "Tunable DFB laser with fan-shaped grating", *Appl. Phys. Lett.*, vol. 31, no. 104, 1977
- [10] E. L. Portnoi, "Semiconductor heterostructure lasers with distributed feedback", *Czech. J. Phys, B*, vol. 34, no. 469, 1984
- [11] P. R. Patterson, D. Hah, M. Fujino, W. Piyawattanametha, and M. C. Wu, “Scanning micromirrors: An overview,” *Proc. SPIE*, vol. 5604, pp. 195–207, Oct. 2004.
- [12] D. Dickensheets and G. Kino, “Micromachined scanning confocal optical microscope,” *Opt. Lett.*, vol. 21, no. 10, pp. 764–766, May 1996.
- [13] A. P. Neukermans and T. G. Slater, “Micromachined torsional scanner,” *U.S. Patent 5 629 790*, May 13, 1997
- [14] Rauch, S. and Sacher, J., “Volume Holographic Grating Stabilized 780nm Ridge Waveguide Laser with an Output Power of 380mW”, *CLEO: Science and Innovations, Paper JTh2A.10* (2015).